www.czasopisma.pan.pl PAN POLSKA AKADEMIA NAUK www.journals.pan.pl

A R C H I V E S O F M E T A L L U R G Y A N D M A T E R I A L S

Volume 59 2014 Issue 3

DOI: 10.2478/amm-2014-0207

M.B. JABŁOŃSKA*

MECHANICAL PROPERTIES AND FRACTOGRAPHIC ANALYSIS OF HIGH MANGANESE STEELS AFTER DYNAMIC DEFORMATION TESTS

WŁAŚCIWOŚCI MECHANICZNE I FRAKTOGRAFICZNA ANALIZA PRZEŁOMÓW STALI WYSOKOMANGANOWYCH PO PRÓBACH DYNAMICZNEJ DEFORMACJI

Since few years many research centres conducting research on the development of high-manganese steels for manufacturing of parts for automotive and railway industry. Some of these steels belong to the group of AHS possessing together with high strength a great plastic elongation, and an ideal uniform work hardening behavior. The article presents the dynamic mechanical properties of two types of high manganese austenitic steel with using a flywheel machine at room temperature with strain rates between $5\times10^2 \div 3.5\times10^3$ s^{-1}. It was found that the both studied steels exhibit a high sensitivity R_m to the strain rate. With increasing the strain rate from 5×10^2 to 3.5×10^3 s^{-1} the hardening dominates the process. The fracture analysis indicate that after dynamic test both steel is characterized by ductile fracture surfaces which indicate good plasticity of investigated steels.

Keywords: high manganese steels, dynamic deformation test, strain rate, fracture

Od kilku lat wiele ośrodków badawczych prowadzi prace nad rozwojem stali wysokomanganowych przeznaczonych do produkcji części dla przemysłu samochodowego i kolejowego. Niektóre z tych stali należą do grupy nazywanej Advanced High Strength Steels, i charakteryzują się wysoką wytrzymałością przy jednocześnie bardzo dużej plastyczności i szerokim zakresie umocnienia. W niniejszej pracy przedstawiono badania właściwości mechanicznych w próbach odkształcenia dynamicznego dla dwóch gatunków wyskomanganowej stali austenitycznej z wykorzystaniem młota rotacyjnego w temperaturze pokojowej z szybkością odkształcenia między $5\times10^2 \div 3{,}5\times10^3$ s^{-1}. Stwierdzono, że badane stale wykazują wysoką czułość wytrzymałości na rozciąganie R_m na prędkość odkształcenia. Wraz ze wzrostem szybkości odkształcenia od 5×10^2 do $3{,}5\times10^3$ s^{-1} następuje proces umocnienia badanych stali. Przeprowadzona analiza faktograficzna przełomów wskazuje, że pękanie po próbach dynamicznej deformacji obu stali ma charakter transkrystaliczny ciągliwy co wskazuje na wysoką plastyczność badanych stali.

1. Introduction

At present, the most important branches of economy, such as automotive, railway and military industries have a need for new materials with much more favorable set of mechanical, plastic and economical properties. A strive for reduction of vehicle mass results in application of various groups of materials, such as composites, polymers or light alloy materials, however the most important elements and those most significant for the safety are as hitherto made of steel. This leads to an essential change in the approach to designing modern steels with wide range of strength and plastics properties. New steels of Fe-Mn-Al group hardened in the result of structural effect induced by plastic deformation may be included into these steels. High-manganese steels are typically austenitic steels, i.e. face-centered cubic (fcc) alloys, with a high Mn content (above 20 wt.%) and additions of elements such as carbon (<1 wt.%), silicon (<3 wt.%) and aluminum (<10 wt.%). [1] These steels include three groups of steels with high-manganese austenitic structure, showing characteristic effects of hardening by deformation, such as transformation-induced plasticity by $\gamma \rightarrow \varepsilon$ martensitic transformation (TRIP) [2,3÷6], twinning-induced plasticity by the formation of deformation twins with nanometer thickness (TWIP) [2,7-12], and microband-induced plasticity by formation the microbands in austenite which are in-grain shear zones that are confined by geometrically necessary boundaries or conventional grain boundaries (MBIP) [13,14]. The effects play a decisive role in formation of extremely favorable connection of mechanical and plastic properties, and their occurrence depends on the criterion of selection of their chemical composition, so as to the activation of these TRIP, TWIP and MBIP mechanisms is strongly dependent on the stacking fault energy [1,15,16]. The value of the stacking fault energy is controlled by the contents of alloying elements; in this relationship, value of $\Delta G\gamma \rightarrow \varepsilon$; difference of molar free energy between the austenite phase and the martensite phase, in relation to the individual alloying elements – is the variable [16]. As it was shown in [15-18], mechanical twins are only formed within a narrow range of SFE values. Allain et al. [16] calculated that twinning can occur for SFEs between 12 and 35 mJ m^{-2}, whereas strain-induced ε martensitic transforma-

* SILESIAN UNIVERSITY OF TECHNOLOGY, FACULTY MATERIALS ENGINEERING AND METALLURGY, INSTITUTE OF MATERIALS SCIENCE, 40-019 KATOWICE, POLAND

tion can occur if the SFE is below 18 mJ m^{-2}. Frommeyer et al. [17] indicated that a SFE larger than about 25 mJ m^{-2} resulted in a twinning effect in a stable austenitic phase, whereas SFEs smaller than about 16 mJ m^{-2} resulted in ε phase formation. Sato et al. [18] reported that a low SFE ($\gamma \leqslant 20$ mJ m^{-2}) favored the $\gamma \rightarrow \varepsilon$ martensitic transformation, while a high SFE (γ >20 mJ m–2) favored deformation twinning instead of martensitic transformation. Dumay et al. [19] indicated that twinning tended to disappear and was replaced by the formation of ε-platelets when the SFE was smaller. Therefore, it is the value of the material factor being the stacking fault energy in the analyzed steels that translates into the ability of the material to harden in the results of controlled structural effects, what is schematically shown in Fig. 1.

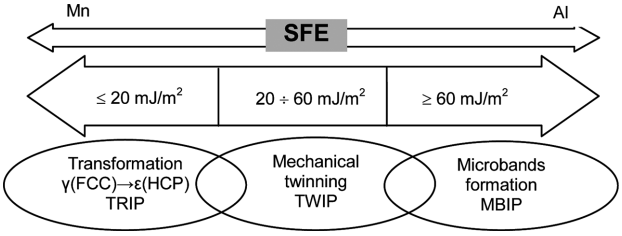

Fig. 1. Schematic presentation of preferred deformation mechanisms depending on SFE changes in high-manganese steels. [Prepared based on 1-19]

The fundamental component controlling stability of austenite during deformation of the discussed steels is manganese. Increase in content of this element leads initially to a decrease in SFE to its minimum value below 5 mJ/m^2, and then to an increase. A high Mn content stabilizes austenite up to room temperature. A fully austenitic structure, containing no martensite and other phases – probable nuclei for breaking – exhibits particularly favorable relationship of strength properties and affinity to plastic working [1-15,20].

While considering TWIP (Twinning Induced Plasticity) steels, which currently may be one of the most prospective materials because of their excellent tensile strength-ductility combination [2,15,24-28], an optimal Mn concentration, favoring generation of the TWIP effect, ranges between 20 and 30 wt.% at the carbon content in the range of 0.03÷0.60 wt.%. Thus, depending on the stability of manganese austenite during deformation, network shearing γ(RSC) may occur by slip, however more frequently by twinning. At the same time, at this Mn content, an introduction of Al to the steel leads to an increase in SFE, and effectively limits $\gamma \rightarrow \varepsilon \rightarrow \alpha$ transformation induced by the deformation, stabilizing high-manganese austenite. This fact also favors deformation hardening in the result of twinning. As for Al, its boundary content resulting to the expected hardening by formation of mechanical twins in manganese austenite, 10 wt.% has been assumed. If the percentage of Al does not exceed this value, then in the SFE range of 20÷60 mJ/m^2, formation of mechanical twins in the austenitic matrix will be the privileged deformation mechanism in the material [1,29]. In the steels containing more than 10 wt.% of Al, the SFE level increases to a value significantly higher than 60 mJ/m^2, and hardening effects in the form of shearing microbands are observed in the microstructure [17,18÷20,26÷32]. The influence of other alloying components on SFE in manganese steels is not so strong.

Another important factor that should be pointed out while discussing materials for the future, is possible safety level which will be achieved in the result of their application. The energy-absorption capacity of TWIP steels may reach 0.5 J/mm3 at 20°C, almost two times higher than that of conventional deep punching steel. Additionally, the TWIP steel has no brittleness transition at low temperature. Till now, most studies are focused on static tests, such as the tensile [2,32,33-36], fatigue [37-39], welding [40], and deformation mechanisms [41,42]. Studies under conditions of dynamic deformations, described in few papers [43,44,45], play an extremely significant role in the case of these steels. However, reports of dynamic mechanical properties of high manganese steel have been relatively few, where the strain rate is from 10^{-5} even to 8000 s^{-1}.We face various kinds of dynamic events in our daily life, the actual engineering projects, military and scientific research – like car accidents, collisions of airplanes with birds, explosions, and so on. The actual strain rate in the above examples is very high. So the dynamic mechanical properties of a high manganese steel under high strain rates are requested [45].

2. Experimental

The high manganese steels used in this study had the chemical composition: Steel1: Fe-27 wt.% Mn-3 wt.% Al-0.3 wt.% C; Steel 2: Fe-30 wt.% Mn-9 wt.% Al-0.6 wt.% C. The steels were prepared in Institute for Ferrous Metallurgy, Gliwice, Poland, in a vacuum induction furnace from Balzers, and they were cast into ingot moulds, obtaining circular ingots with a mass of about 25 kg. The ingots were subjected to homogenizing annealing at 1170°C for 3 h. The batches were heated uniformly and annealed through. Then, they were subjected to open die forging by press forging and hammer forging. The hot-rolled steel 1 showed a fully austenitic structure with an average grain sizes of 53 mm and 48 mm, which remained stable during deformation at room temperature. The steel 2 showed an austenitic-ferritic structure with 22% area fraction of ferrite. Based on the chemical composition of the investigated steels, the stacking fault energy has been estimated by thermodynamic calculations [22]. The stacking fault energy of examined steels are summarized in Table 1.

TABLE 1

Examined SFE of researched steels

Steel grade	steel 1 Fe-27 wt.% Mn-3 wt% Al-0.3 wt.% C	steel 2 Fe-30 wt.% Mn-9 wt% Al-0.6 wt.% C
SFE, mJ/m^2 (estimated by thermodynamic calculations)	25	84

Studies of dynamic deformation were carried out using a flywheel machine type RSO from WPM Lipsk, owned by Institute of Materials Technology of Silesian University of Technology for linear velocities of v = 7.5, 15, and 30 m/s. Based on force characteristics and measurements of the sample's geometry before and after the deformation, the following

parameters were determined: strain rate , tensile strength R_m, maximum deformation ε_g. The device enables deformation, tensile, and bending of samples with linear impact rate in the range of 5÷40 m/s, corresponding to strain rates in the range of 102÷104 s-1. During the dynamic tensile tests, the sample being tensile is connected with the top holder, and it is subjected to a deformation by an impact of the swingle in the anvil of the bottom holder. The exchangeable claw is installed on a flywheel with a very high moment of inertia. The measurement of force during tensile tests is carried out based on an extensometric force sensor with a rated range of 25 kN, having a design adjusted to the installation in stand or anvil elements, depending on the character of the test being carried out. For measurement of the deformation of the sensor's elastic element, extensometers of 0,6/120 LY11 type from Hottinger Baldwin Messtechnik were used, connected as a complete bridge system.

Then, the linear rate of the swingle in the discussed measurement system was determined by a measurement of rotational speed of the hammer's flywheel. The rate measurement was carried out using an encoder installed in the tip of the pivot of the hammer's shaft, having its stator connected with the hammer's structure by a coupling device with a static coupling, ensuring a high torsional rigidity of the connection. The encoder has a working resolution in the range of 3600 imp./rev., translating into distinguishing of about 0.5-mm path on the radius of the hammer's swingle. The linear rate of the swingle was determined by estimation of the frequency of the rectangular wave at the output of the encoder. In the tests, cylindrical smooth samples with a diameter of 4 mm and a length of the measurement part of 20 mm, bilaterally threaded in the holder part were used. During the tests, the course of the tensile force vs. time and the linear rate of the swingle installed in a flywheel, were recorded. The recording time of the measurement signal in the system was 10 s. The following parameters may be determined from the force characteristics and the measurements of geometry of the sample before and after the deformation: tensile strength R_m, maximum deformation εg, strain rate, impact resistance U. The fracture structures after dynamic tests was analyzed by scanning electron microscopy (SEM).

3. Results

The results of dynamic tensile tests obtained for all analyzed steels are shown in Figures 6, 7, 8. Fig. 6 shows a dependence between the linear rate of the swingle and the average strain rate. The strain rates (strain rate) in the studied samples is in the range of $5\times10^2 \div 3.5\times10^3$ s-1. While analyzing Fig. 7, it may be ascertained that a decrease in the value of maximum deformation with an increase in the swingle's linear rate occurs for Steel 2. For Steel 1, there is no such tendency. The maximum deformation maintains an almost constant level, and even increases for a velocity of 30 m/s, while compared to that for a velocity of 15 m/s. It may indicate a very high plasticity reserve of the studied steel. The courses of tensile strength of the investigated steels is shown in Fig. 7. Both studied steels exhibit a high sensitivity R_m to the strain rate. Steel 2 has the highest sensitivity to the strain rate. Also the value of the tensile strength of Steel 2 is higher than those of the Steel 2 in the whole range of the strain rate. The maximum deformation of Steel 2 displays a falling tendency, and increase of Steel 1, the maximum deformation remains constant. One may ascertain that Steel 2 exhibits a higher influence of the strain rate on the tensile strength. The tensile strength of Steel 2 is significantly higher than those of Steel 1.

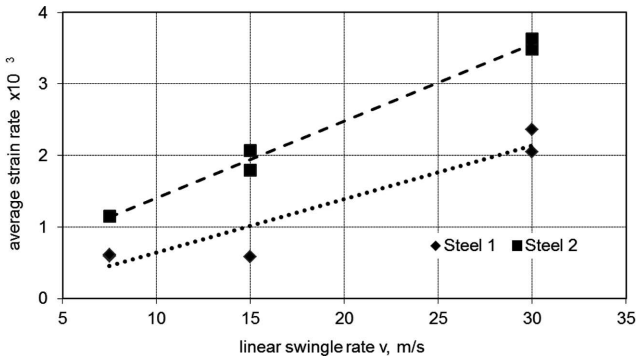

Fig. 2. Dependence between the swingle linear velocity and the average strain rate

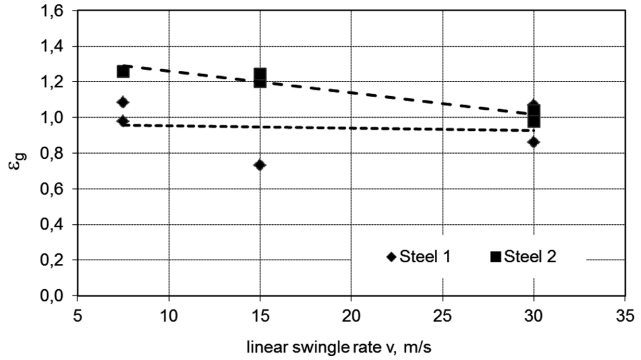

Fig. 3. Influence of the swingle linear velocity on the maximum deformation

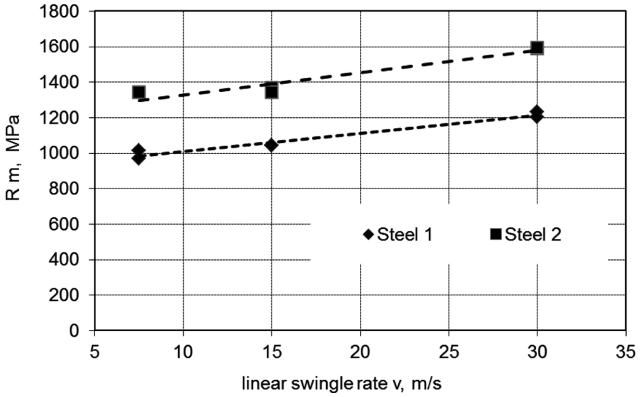

Fig. 4. Influence of the swingle linear velocity on the tensile strength

After dynamic tensile tests with a velocity of 30 m/s, observations of fractures were carried out for all steels in order to determine their cracking ability. All studied steels exhibit a ductile form of fractures, irrespective of the swingle linear velocity applied (Figs. 9, 10). In both studied steels, fractures with characteristic crater structure were observed. Structural analysis of surfaces of the fractures showed a presence of voids typical for transcrystalline ductile cracking mechanism.

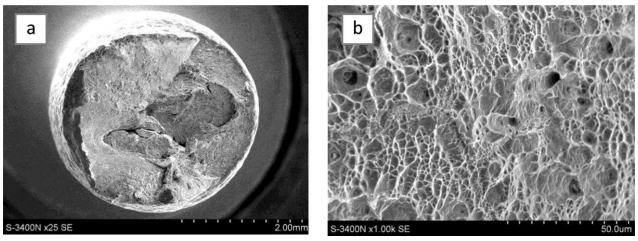

Fig. 5. Steel 1 after dynamic tensile tests, a) view of the surface of the sample, b) ductile fracture surface with a fine crater structure

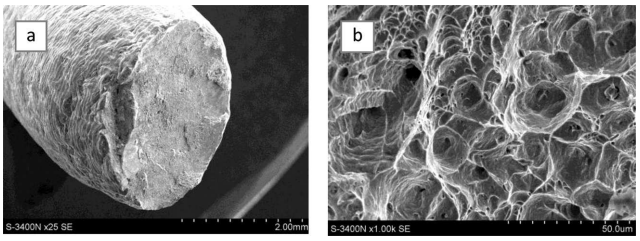

Fig. 6. Steel 2 after dynamic tensile tests, a) view of the surface of the sample, b) ductile fracture surface with a deep crater structure

4. Conclusions

We studied the effects of strain rates on the mechanical properties of the two types of high manganese steels under the impact tests at room temperature. The steels has different SFE value which is due to different contents of the basic elements such as Mn and Al. The differences in the value of SFE indicate that Steel 1 should be characterized by the occurrence of the TWIP effect, and Steel 2 would show the MBIP effect.

I was found that for Steel , the maximum deformation maintains an almost constant level. Increases for a strain rate was not decrease in. For Steel 2, there is no such tendency, with an increase in the swingle's linear rate the value of maximum deformation decrease. However, both exhibit a very high plasticity reserve. The studied steels exhibit a high sensitivity R_m to the strain rate. The value of the tensile strength of Steel 2 is higher than those of the Steel 1 in the whole range of the strain rate. The obtained results were confirmed by observations of fracture of tested steels. In all tested samples were observed ductile form of fractures, with characteristic crater structure.

All these parameters obtained in this study could lead to the utilization of the high manganese steel in the engineering applications.

Acknowledgements

The author would like to thank Dr hab. inż. Grzegorz Niewielski, Prof. Pol. Śl., Prof. dr hab. inż. Eugeniusz Hadasik and Dr hab. inż. Jacek Pawlicki, Prof. Pol. Śl., for supporting the research, leading to this results. Financial support of BK232/RM3/2014 is gratefully acknowledged.

REFERENCES

[1] I. Gutierrez-Urrutia, D. Raabe, Acta Mater. **59**, 6449 (2011).
[2] O. Grässel, L. Krüger, G. Frommeyer, L.W. Meyer, Int. J Plast. **16**, 1391 (2000).
[3] Y. Lu, B. Hutchinson, D.A. Molodov, G. Gottstein, Acta Mater. **58**, 3079 (2010).
[4] A. Grajcar, M. Opiela, G. Fojt-Dymara, Arch. of Civil and Mech. Eng. **9**, 3, 49 (2009).
[5] D. Dziedzic, K. Muszka, J. Majta, Arch. Of Metal. And Mater. **58**, 3, 745 (2013).
[6] S. Wiewiórowska, Arch. of Metal. And Mater. **58**, 2, 574 (2013).
[7] J.E. Jin, Y.K. Lee, Mater. Sci. Eng. A **527**, 157 (2009).
[8] J.K. Kim, L. Chen, H.S. Kim, S.K. Kim, Y. Estrin, B.C.D. Cooman, Metall. Mater Trans A **40**, 3147 (2009).
[9] S. Curtze, V.T. Kuokkala, Acta Mater. **58**, 5129 (2010).
[10] I. Gutierrez-Urrutia, S. Zaefferer, D. Raabe, Mater Sci. Eng. A **527**, 3552 (2010).
[11] H. Idrissi, K. Renard, D. Schryvers, P.J. Jacques, Scripta Mater. **63**, 961 (2010).
[12] Y. Lu, D.A. Molodov, G. Gottstein, Acta Mater. **59**, 3229 (2011).
[13] J.D. Yoo, K.T. Park, Mater Sci. Eng. A **496**, 417 (2008).
[14] J.D. Yoo, S.W. Hwang, K.T. Park, Metall. Mater Trans A **40**, 1520 (2009).
[15] L. Remy, A. Pineau, Mater. Sci. Eng. **28**, 99 (1977).
[16] S. Allain, J.-P. Chateau, O. Bouaziz, S. Migot, N. Guelton, Mater. Sci. Eng. A **387-389**, 158 (2004).
[17] G. Frommeyer, U. Brux, P. Neumann, ISIJ Inter. **43**, 438 (2003).
[18] K. Sato, M. Ichinose, Y. Hirotsu, Y. Inoue, ISIJ Inter. **29**, 868 (1989).
[19] A. Dumay, J.-P. Chateau, S. Allain, S. Migot, O. Bouaziz, Mater. Sci. Eng. A **483-484**, 184 (2008).
[20] O. Bouaziz, S. Allain, C.P. Sccot, P. Cugy, D. Barbier, Opinion in Solid State and Materials Science **15**, 141 (2011).
[21] S.A. Hamada, Acta Universitatis Ouluensis, C281, 2007.
[22] W. Bleck, Effect of Microalloying in Multi Phase Steels for Car Body Manufacturing, 14 Sächsische Fachtagug Umfortechnik, Freiberg, 2007.
[23] F. Grosman, R. Kawalla, Modern constantly on the sheet for the automotive industry, collective work Hadasik E. Processing of Metal Plasticity and Structure.
[24] G. Frommeyer, U. Brüx, Steel Research International **77**, 627 (2006).
[25] O. Grässel, G. Frommeyer, C. Derder, H. Hofmann, J Physique IV **7**, C5, 383 (1997).
[26] A. Prakash, T. Hochrainer, E. Reisacher, H. Riedel, Steel Research International **79**, 8, 645 (2008).
[27] H. Schuman, Neue Hutte **17**, 605 (1971).
[28] T.W. Kim, Mat. Sci. Eng. A **160**, 13 (1993).
[29] M. Jabłońska, and A. Śmiglewicz, Defect and Diffusion Forum **334-335**, 177 (2013).
[30] Y. Kim, N. Kang, Y. Park, I. Choi, G. Kim, S. Kim, K.J. Cho, Kor. Inst. Met. Mater. **46**, 780 (2008).
[31] Y.G. Kim, J.M. Han, J.S. Lee, Mater. Sci. Eng. A **114**, 51 (1989).
[32] B.W. Oh, S.J. Cho, Y.G. Kim, Y.P. Kim, W.S. Kim, S.H. Hong, Mater. Sci. Eng. A **197**, 147 (1995).
[33] R. Ueji, N. Tsuchida, D. Terada, N. Tsuji, Y. Tanaka, A. Takemura, K. Kunishige, Scr. Mater. **59**, 963 (2008).
[34] D. Barbier, N. Gey, S. Allain, N. Bozzolo, M. Humbert, Mater. Sci. Eng. A **500**, 196 (2009).
[35] J.D. Yoo, S.W. Hwang, K.-T. Park, Mater. Sci. Eng. A **508**, 234 (2009).

[36] A.S. Hamada, L.P. Karjalainen, Mater. Sci. Eng. A **528**, 1819 (2011).
[37] T. Niendorf, C. Lotze, D. Canadinc, A. Frehn, H.J. Maier, Mater. Sci. Eng. A **499**, 518 (2009).
[38] T. Niendorf, F. Rubitschek, H.J. Maier, J. Niendorf, H.A. Richard, A. Frehn, Mater. Sci. Eng. A **527**, 2412 (2010).
[39] A.S. Hamada, L.P. Karjalainen, Mater. Sci. Eng. A **527**, 5715 (2010).
[40] L. Mujica, S. Weber, H. Pinto, C. Thomy, F. Vollertsen, Mater. Sci. Eng. A **527**, 2071 (2010).
[41] T.A. Lebedkina, M.A. Lebyodkin, J.P. Chateau, A. Jacques, S. Allain, Mater. Sci. Eng. A **519**, 147 (2009).
[42] A. Soulami, K.S. Choi, Y.F. Shen, W.N. Liu, X. Sun, M.A. Khaleel, Mater. Sci. Eng. A **528**, 1402 (2011).
[43] D.Z. Li, Y.H. Wei, C.Y. Liu, L.F. Hou, D.F. Liu, X.Z. Jin, J. Iron Steel Res. Int. **17**, 67 (2010).
[44] R.-G. Xiong, R.-Y. Fu, Y. Su, Q. Li, X.-C. Wei, L. Li, J. Iron Steel Res. Int. **16**, 81 (2009).
[45] Z.-P. Xiong, X.-P. Ren, W.-P. Bao, S.-X. Li, H.-T. Qu, Mater. Sci. Eng. A **530**, 426 (2011).

Received: 20 March 2014.